

# DESIGN AND BEAM TEST OF SIX-ELECTRODE BPMS FOR SECOND-ORDER MOMENT MEASUREMENT

K. Yanagida\*, S. Suzuki, and H. Hanaki, JASRI/SPring-8, Sayo Hyogo, Japan

## Abstract

To enhance a beam observation system during top-up operation, we developed in the SPring-8 linear accelerator non-destructive beam position monitors (BPMS) that can detect second-order moments of electron beams. BPMS have six stripline-type electrodes with circular or quasi-elliptical cross-sections. We tested a BPM with a circular cross-section using electron beams, and our results showed that its normalized moments were determined accurately by electrostatic field calculation. We studied a precise calibration method to determine the relative attenuation factors between the electrode channels based on the principle that the relative moments must not vary with a change of the beam position using a steering magnet in drift space.

## INTRODUCTION

The SPring-8 linear accelerator provides electron beams toward a storage ring about every twenty seconds because of the top-up operation of the storage ring. To enhance the beam observation system during the top-up operation, a non-destructive BPM system is being upgraded to a six-electrode BPM system that can detect the second-order moments of electron beams because the second-order moments are physical quantities related to beam sizes, which can be deduced by measuring second-order moments at more than six locations in FODO magnetic lattices [1].

Therefore, we developed the major components of a six-electrode BPM system: BPMS, a signal processor, and a digital input board. We installed our developed six-electrode BPMS with a circular cross-section in the beam transport line and tested them using electron beams. This paper describes the BPM designs as the parts of the six-electrode BPM system, the principle of multipole moment measurement, and the beam test results.

## SIX-ELECTRODE BPMS

This section describes the designs of six-electrode BPMS and the principle of absolute moment measurement.

### BPM designs

We developed two kinds of six-electrode BPMS for second-order moment measurement. One is a BPM with a circular cross-section for the non-dispersive section, and the other is a BPM with a quasi-elliptical cross-section for the dispersive section (Fig. 1). In the figure the numbers represent electrode number  $d$ . Both BPMS have stripline-type electrodes as signal pick-ups. The stripline length is

27 mm, which corresponds to  $\lambda/4$  of the acceleration radio frequency. The characteristic impedance is designed as  $50 \Omega$ . One electrode of both BPMS shares  $30^\circ$  with respect to the duct center. The aperture radius of a BPM with a circular cross-section is 16 mm, and the long and short radii of a BPM with a quasi-elliptical cross-section are 14 mm and 28 mm. These BPMS were or will be installed instead of the existing four-electrode BPMS with circular and quasi-elliptical cross-sections [2][3].

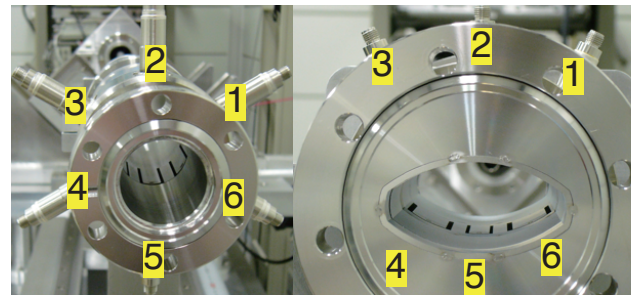


Figure 1: Six-electrode BPMS with circular and quasi-elliptical cross-sections. Numbers represent electrode number  $d$ .

### Absolute Moment Measurement

A BPM with symmetrical arranged electrodes can detect multipole moments with respect to the duct center. These are called absolute moments  $P_n$  and  $Q_n$ , where  $n$  is the order of the multipole moment. For example, first-order absolute moments represent the transverse positions of beam centroid  $P_1$  (horizontal position) and  $Q_1$  (vertical position). The two-dimensional position  $(P_1, Q_1)$  is generally called the beam position.

Our developed six-electrode BPMS have two electrodes in the vertical direction, but none horizontally. This configuration enables us to measure three higher-order ( $n \geq 2$ ) absolute moments:  $P_2$ ,  $Q_2$ , and  $Q_3$ .

Because the signal voltage of each electrode  $V_d$  is proportional to the integral of the electric field strength on the electrode, we can obtain the absolute moments with normalized moments  $R_{P_n}^n/2$ ,  $R_{Q_n}^n/2$  and geometrical factors  $k$ ,  $K$ , as described in Eq. (1). In the equation,  $R_{P_n}$  or  $R_{Q_n}$  is called an effective aperture radius. The effective aperture radii and the geometrical factors are calculated analytically, especially for a BPM with circular cross-section, or numerically [4].

The calculation result is summarized in Table 1. A smaller effective aperture radius is preferable for accurate

\*ken@spring8.or.jp

measurement, but  $R_{Q1}$  is rather large:

$$\begin{aligned}
 P_1 &= \frac{R_{P1}}{2} \frac{V_1 - V_3 - V_4 + V_6}{V_1 + V_3 + V_4 + V_6}, \\
 Q_1 &= \frac{R_{Q1}}{2} \frac{V_1 + V_3 - V_4 - V_6}{V_1 + V_3 + V_4 + V_6}, \\
 P_2 &= \frac{R_{P2}^2}{2} \frac{kV_1 - 2V_2 + kV_3 + kV_4 - 2V_5 + kV_6}{kV_1 + 2V_2 + kV_3 + kV_4 + 2V_5 + kV_6}, \\
 Q_2 &= \frac{R_{Q2}^2}{2} \frac{V_1 - V_3 + V_4 - V_6}{V_1 + V_3 + V_4 + V_6}, \\
 Q_3 &= \frac{R_{Q3}^3}{2} \frac{KV_1 - V_2 + KV_3 - KV_4 + V_5 - KV_6}{KV_1 + V_2 + KV_3 + KV_4 + V_5 + KV_6}.
 \end{aligned} \quad (1)$$

Table 1: Effective aperture radii and geometrical factors

	circular (analytical)	quasi-elliptical (numerical)
$R_{P1}$ [mm]	18.69	18.03
$R_{Q1}$ [mm]	32.38	54.84
$R_{P2}$ [mm]	18.91	18.42
$R_{Q2}$ [mm]	17.59	22.48
$R_{Q3}$ [mm]	16.57	18.55
$k$	1.000	1.918
$K$	1.000	3.056

## RELATIVE MOMENTS

As described above, the absolute moments of six-electrode BPMs can be obtained using Eq. (1). However, they are rather complicated because they involve not only the moments of a beam intensity distribution called relative moments  $P_{gn}$  and  $Q_{gn}$  but also the moments of the beam centroid. For easier comparison of the multipole moments, we define the relative moments and extract them from the absolute moments.

Relative moments are defined as the moments with respect to the beam centroid. It is considered that the origin is transferred from the duct center (0, 0) to the beam position ( $P_1$ ,  $Q_1$ ) to cancel the first-order relative moments, i.e.,  $P_{g1}=0$  and  $Q_{g1}=0$ . Consequently, we can obtain the relative moments from the absolute moments using the following relations [4]:

$$\begin{aligned}
 P_1 &= b_G \cos \beta_G, \quad Q_1 = b_G \sin \beta_G, \\
 P_{g2} &= a_{g2}^2 \cos 2\alpha_{g2} = P_2 - b_G^2 \cos 2\beta_G, \\
 Q_{g2} &= a_{g2}^2 \sin 2\alpha_{g2} = Q_2 - b_G^2 \sin 2\beta_G, \\
 Q_{g3} &= Q_3 - b_G^3 \sin 3\beta_G - 3b_G a_{g2}^2 \sin(\beta_G + 2\alpha_{g2}).
 \end{aligned} \quad (2)$$

## SCREEN MONITOR FOR RELATIVE MOMENT MEASUREMENT

At the beam test, the relative moments were also measured by a screen monitor that records the two-dimensional beam intensity distribution on the screen (DESMAR-QUEST AF995R) into the intensity distribution on a

03 Technology

3G Beam Diagnostics

charge-coupled device (CCD) using an optical focusing lens when the electron beams hit the screen.

We define the intensity distribution on the screen as  $I(x_i, y_j)$ , where  $x_i$  and  $y_j$  indicate the position of the data cell. The origin is defined as the screen center, i.e., the duct center, but not the CCD center. To calculate the absolute moments from  $I(x_i, y_j)$ , we define  $n$ th-order absolute intensity moments  $m_{h(n-h)}$  in the Cartesian coordinates, as described in Eq. (3), and consequently obtain the absolute moments using Eq. (4) [4]:

$$\begin{aligned}
 m_{00} &= \sum_i \sum_j I(x_i, y_j), \quad m_{10} = \sum_i \sum_j x_i I(x_i, y_j), \\
 m_{01} &= \sum_i \sum_j y_j I(x_i, y_j), \quad m_{20} = \sum_i \sum_j x_i^2 I(x_i, y_j), \\
 m_{11} &= \sum_i \sum_j x_i y_j I(x_i, y_j), \quad m_{02} = \sum_i \sum_j y_j^2 I(x_i, y_j), \\
 m_{21} &= \sum_i \sum_j x_i^2 y_j I(x_i, y_j), \quad m_{03} = \sum_i \sum_j y_j^3 I(x_i, y_j).
 \end{aligned} \quad (3)$$

$$\begin{aligned}
 m_{00}P_1 &= m_{10}, \quad m_{00}Q_1 = m_{01}, \\
 m_{00}P_2 &= m_{20} - m_{02}, \quad m_{00}Q_2 = 2m_{11}, \\
 m_{00}Q_3 &= 3m_{21} - m_{03}.
 \end{aligned} \quad (4)$$

Figure 2 shows the example data of the beam intensity distribution (contour plot) on the screen. Using Eqs. (3) and (4), the multipole moments of this distribution were obtained as  $P_1=2.334$  mm,  $Q_1=-0.989$  mm,  $P_{g2}=-0.391$  mm<sup>2</sup>,  $Q_{g2}=1.366$  mm<sup>2</sup>, and  $Q_{g3}=0.161$  mm<sup>3</sup>.

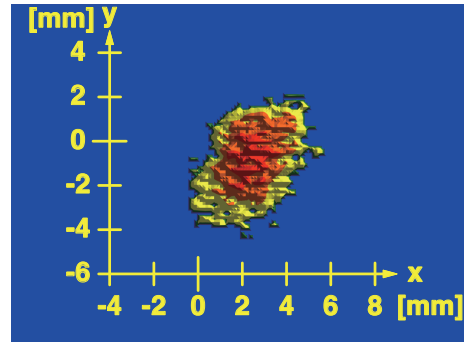


Figure 2: Two-dimensional beam intensity distribution (contour plot) on screen

## BEAM TEST

We performed a beam test of a six-electrode BPM with a circular cross-section to verify whether the normalized moments measured by the beam test agree with those calculated analytically.

### Entire Calibration

Even though each element of the system is calibrated precisely, entire calibration is very difficult and is not eas-

ISBN 978-3-95450-122-9

ily achieved. To resolve this problem we studied a method for entire calibration using electron beams.

The principle is very simple. We assume that the electron beams are stable during the beam test and that the steering magnets change the beam position without changing the beam intensity distribution with respect to the beam centroid. If we change the beam position at the BPM location using upstream steering magnets, observed relative moments  $P_{g2}$ ,  $Q_{g2}$  and  $Q_{g3}$  must be constant. Conversely speaking, we can easily determine the relative attenuation factors between the electrode channels so that all the obtained relative moments are constant.

After we determined the relative attenuation factors, we applied them to all the data including the entire calibration data. Figure 3 shows example data of the multipole moments of the entire calibration. The beam position ( $P_1$ ,  $Q_1$ ) and second-order absolute moments  $P_2$  vary by means of steering magnets, but second-order relative moments  $P_{g2}$  do not.

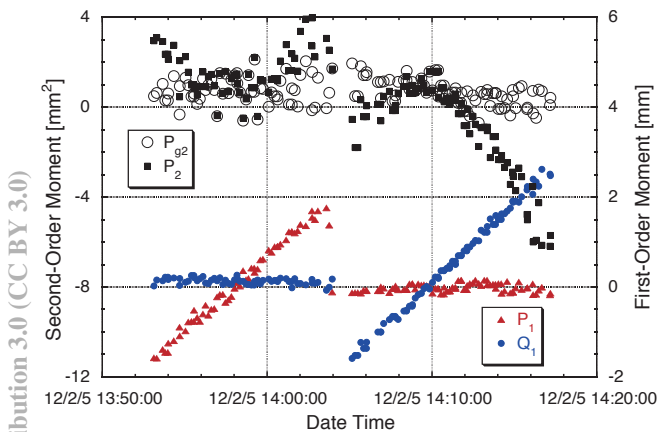


Figure 3: Multipole moments of entire calibration. Relative attenuation factors are applied.

### Correlation Measurement

Finally, we compared the second-order relative moments taken by the screen monitor to those by the BPM when we changed the beam intensity distribution by changing the magnetic field of the upstream quadrupole magnet. Because the screen monitor was located upstream of the BPM in the drift space, we did not take both bits of data at the same beam shot. The distance between the screen monitor and the BPM is  $\sim 2$  m.

Figure 4 is the correlation plot between the second-order relative moments taken by the screen monitor (abscissa) and the BPM (ordinate). In the plot the spread data points were caused by the shot by shot fluctuation of the beam intensity distribution. However, the correlation plot apparently indicates a direct proportionality relation with a proportionality coefficient of 1.

This result provides the following important consequences. One, for such BPMs with stripline-type electrodes, normalized moments can be obtained accurately by

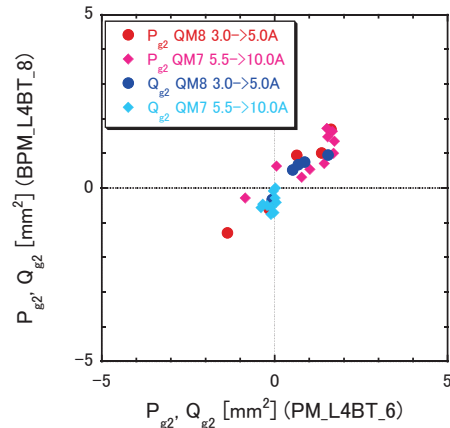


Figure 4: Correlation plot between second-order relative moments taken by screen monitor (abscissa) and BPM (ordinate)

analytical or maybe numerical electrostatic field calculation, i.e., the correlation plot with a proportionality coefficient of 1. The other is that an entire calibration is useful as is a self-consistent method for precise calibration to determine the relative attenuation factors between electrode channels, i.e., the correlation plot passing through the origin.

## SUMMARY

We developed six-electrode beam position monitors with circular and quasi-elliptical cross-sections for second-order moment measurement. From the beam test results normalized moments of BPM with circular cross-section were accurately determined by analytical electrostatic field calculation. The entire calibration is useful and a self-consistent method for precise calibration to determine the relative attenuation factors between electrode channels.

## REFERENCES

- [1] R. H. Miller, et al., "Nonintercepting Emittance Monitor," Proc. 12th Int. Conf. High-Energy Accel. (HEAC'83), Fermilab USA, 1983, pp. 603-605.
- [2] K. Yanagida, et al., "A BPM System for The SPring-8 Linac", Proc. of the 20th Int. Linac Conf., Monterey USA, Aug. 2000, pp. 190-192.
- [3] K. Yanagida, et al., "Beam Instrumentation Using BPM System of The SPring-8 Linac," Proc. of the 22th Int. Linac Conf., Lubeck Germany, Aug. 2004, pp. 438-440.
- [4] K. Yanagida, et al., Phys. Rev. ST Accel. Beams **15**, 012801 (2012).